

# We are IntechOpen, the world's leading publisher of Open Access books Built by scientists, for scientists

6,200

Open access books available

169,000

International authors and editors

185M

Downloads

Our authors are among the

154

Countries delivered to

TOP 1%

most cited scientists

12.2%

Contributors from top 500 universities



WEB OF SCIENCE™

Selection of our books indexed in the Book Citation Index  
in Web of Science™ Core Collection (BKCI)

Interested in publishing with us?  
Contact [book.department@intechopen.com](mailto:book.department@intechopen.com)

Numbers displayed above are based on latest data collected.  
For more information visit [www.intechopen.com](http://www.intechopen.com)



## Chapter

# Numerical Analysis of the Steady State in SAW Sensor Structures with Selected Polymers for Detection of DMMP and CO

*Tomasz Hejczyk, Jarosław Wrotniak and Wiesław Jakubik*

## Abstract

The chapter presents the results of the numerical investigation of the SAW gas detector structures with selected polymer layers in steady-state conditions. The effect of SAW velocity changes vs. the surface electrical conductivity of the detector structures is predicted on the base of acoustoelectric elemental theory. The electrical surface conductivity of the rough polymer sensing layer placed above the piezoelectric waveguide depends on the profile of the diffused gas molecule concentration inside the whole detector structure. Numerical results in the steady state conditions for the gas molecules DMMP and polymer layer of (RR)-P3HT have been shown as well as for carbon oxide molecules with thin polyaniline and polypyrrole layer. The main aim of the investigations was to study a thin film's interaction with targeted gases in the SAW detector configuration based on diffusion equations for polymers. Numerical results for profile concentration in steady state conditions for gas molecules concentration, film thickness, roughness, and interaction temperature have been shown. The results of numerical analyzes allow for selecting better detector design conditions, including the morphology of the detector layer, its thickness, operating temperature, and layer type. The numerical results, based on the code written in Python, were shown.

**Keywords:** SAW (surface acoustic wave) gas detector, SAW, DMMP (dimethyl methylphosphonate) detection, polymer, (Regio-regular)-P3HT, (RR)-P3HT, polyaniline (PANI), polipirol (PPy), Nafion, numerical acoustoelectric analysis (NAA), Ingebrigtsen's formula, CO (carbon monoxide), python

## 1. Introduction

Polymers are a very interesting material for testing the concentration of particularly dangerous gases, CO (the silent killer), and are also used in research on toxic warfare agents. The following publication presents two approaches that have evolved during research, both in terms of the laboratory method—optimization of the measurement system in terms of control, and thanks to technological progress and the use of atomic force microscopy (AFM). This lastly allows for the emergence of the

polymer structure and confirmation of the dependence of the shape of the detector surfaces, its morphology, and its influence on the SAW detector response. Historically, different thin film materials and the piezoelectric substrates ( $\text{LiNbO}_3$ —lithium niobate Y cut-Z propagation) were utilized with the detector layers ranging from semiconducting to polymers—on which we focused in our research work—PANI (polyaniline), PPY (polypyrrole) with NAFION—to detect carbon oxide (CO), and RR-P3HT (regio-regular poly-3-hexylthiophen)—to detect DMMP (dimethylomethylphosphonate) [1]—a simulant of the poison of chemical warfare agent (CWA), like sarin. The development and optimization of the NNA direction (normalized numerical acoustoelectric analysis) over the analytical detector with an acoustic surface wave (SAW), which now, thanks to technological development, has been empirically confirmed.

Over the decade, the research team made efforts to select the appropriate detector layer, its thickness, porosity, and morphology for individual gases that are important for human safety, e.g. in CO detectors [2]. This publication was created from these research works. Particular importance, also from the point of view of safety, are polymer layers, those photoconductive, which are used to detect CWA (Chemical Warfare Agents), the use of which in systems can significantly prevent a tragedy. For the purposes of the experiment, an original analytical model of the gas detector was created. Initially, this model was based on Knudsen diffusion mechanisms and was inspired by the works of: Matsumaga N., Sakai G., Shimano K., Yamazoe N [3, 4]. The main aim of the investigation was to study thin film interaction with target gases in the SAW detector based on a simple reaction-diffusion eq. [5–11]. Diffusion equations provide theoretical bases for the analysis of physical phenomena like heat transport or mass transport in porous, roughness substrates [5].

In the initial version of the development of the analytical model, the porosity of the layer was taken into consideration. This model was a good illustration of the operation of semiconductor gas detectors. However, in the case of polymer layers and due to different physicochemical properties [12] of polymer layers and other differential equations, this model had to evolve toward a model that took into account the roughness of the layer.

Generally, these detectors have a very high sensitivity, much higher than the commercially available resistance gas detector. Detectors based on surface acoustic waves are widely used in many industries, especially in biochemical applications, allowing for monitoring of DNA mutation [13] and commercial applications, such as monitoring the quality of food, as well as monitoring the physical and chemical properties of solids, such as adsorption/desorption of the substance, humidity.

The chapter summarizes the acoustoelectric theory, i.e. Ingebrigtsen's formula, dynamics gas diffusion concentration profiles in steady-state, and predicts the influence of a thin polymer detector layer with new polymer gas diffusion model on the SAW wave velocity in a piezoelectric acoustic waveguide [14].

Delay lines, with acoustic surface wave (SAW), enable the detection of very small concentrations of chemical compounds in gas mixtures [15]. The miniaturization of these transducers resulted in a significant increase in the frequency of SAW detector. However, miniaturization of the detector requires the construction of more complicated or technically advanced electronic devices (**Figure 1**), while the test and measurement system for gas detection [6, 17–20] has been designed and developed independently.

The detection materials used here, such as DMMP, are not only valuable due to the fact that they can be used as sarin simulants for the calibration of organophosphorus

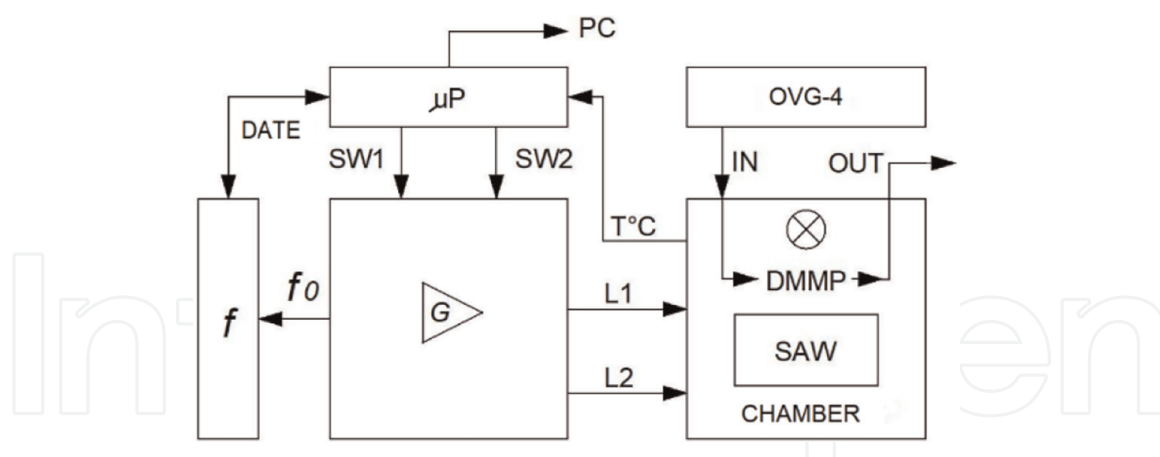


**Figure 1.** Measurement appliance—patent no PAT.230526—system for detecting chemical compounds in gaseous atmospheres, with a detector using surface acoustic waves (SAW) and digital switches SW1 and SW2 ([16],  $\mu\text{P}$ —microprocessor, OVG-4—the owlstone calibration gas generator, G—generator design and implementation by authors: J. Wrotniak and M. Magnuski).

detectors, but also due to the obvious fact that DMMP can be used in the production of chemical weapons (sarin and soman) and is applicable to the construction of very sensitive detectors of this unnoticeable lethal weapon—chemical weapon, which in war conditions (in violation of international rules of war) has a special military and strategic importance.

Chemical warfare agents (CWA), especially nerve agents (e.g. sarin and soman) are highly lethal compounds. Sarin is one of the best-known chemical weapons of mass destruction. This odorless and colorless compound causes neuromuscular paralysis and death by suffocation within 1–10 min. Disabling and lethal exposures to sarin occur above 15 ppb and 64 ppb, respectively for 10 min of exposure [21].

In gas detectors based on SAW, the mechanism of detecting the concentration of the gas or vapors of a chemical compound depends on the interaction of its molecules with a properly selected detector layer sensitive to its presence [22]. The processes of interaction between gas molecules with the layer are kinetic phenomena, mainly sorption (in volume) and adsorption (on the surface), resulting from the entrapment of the molecule in the layer or on its surface. Sorption of gas or vapor molecules through the detector layer causes a change in its mass and electrical conductivity (change in conductivity affects the change of SAW propagation velocity) which in the measurement system leads to a change in the generator's operating frequency [23]. The channel with the detector layer generates as a result oscillations with a different frequency (usually lower) and is shifted in phase relative to the signal generated in the reference path (**Figure 2a**). The work focused on the electrical effect is a new contribution to the SAW gas detector technology [7].

The results of the research on the application of RR-P3HT (poly 3-hexylthiophene regioregular type) produced by means of air spraying on a quartz module with SAW 205 MHz to detect traces of DMMP (Dimethyl methylphosphonate) molecules were presented [1, 15]. DMMP is a non-toxic substance with a similar chemical structure to sarin (Combat Poisoning Agent) and it allows for safe experiments.

Due to the photoconductive properties of the P3HT polymer [24], the layer was additionally activated by LED light (**Figure 2b**). The sensitivity of the layer in the system with SAW [25] to the presence of DMMP in this manner was increased (different wavelengths of LED illumination). Oscillations (in reference and measurement line) were excited. Generator 205 MHz with switched channels was used.

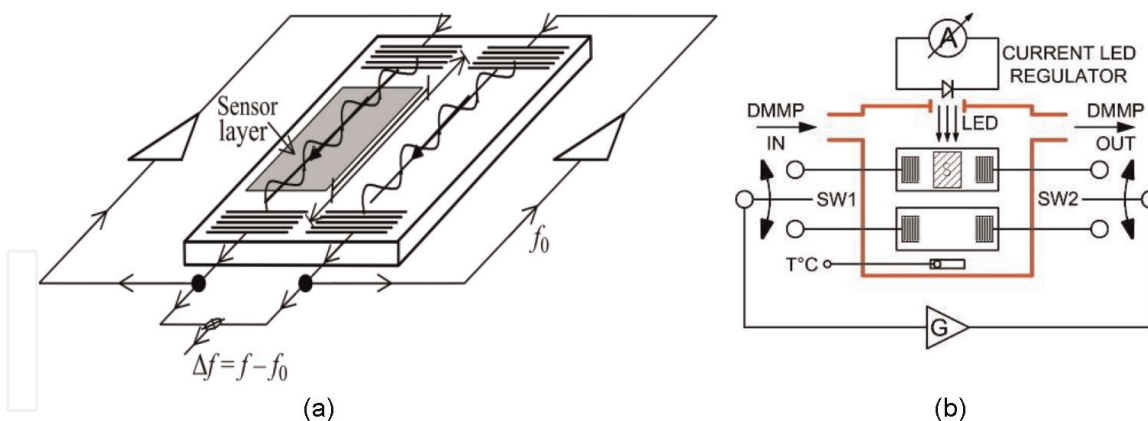


**Figure 2.** Measuring appliance: (a) the idea of the historical measuring system [2, 14], and (b) the newest measurement system with LED lighting with switched channels [1, 8, 16].

The essence of the conducted research is the search for new materials and ways to activate them in order to detect trace concentrations of DMMP in the air without the need of applying high temperatures (above 100°C) [1].

## 2. Technology of applying the detector layer PANI and (RR)—P3HT and sensing mechanism

The bilayer structure of Nafion-Polyaniline was examined by the acousto-electric method (**Figure 2a**). An electrometer Keithley was used in the study due to the high resistance of the structure. The main purpose of the Nafion application was the possibility of controlled protonation of the second layer based on polyaniline to increase its electrical conductivity. Nafion (thickness of approx. 300 nm) and polyaniline (for the thickness of the layers: 100, and 180 nm) were used as sensing structures [2]. A thin layer of Nafion was deposited on the surface of the  $\text{LiNbO}_3$  waveguide by the spin-coating method at speed of 7500 rpm. Thin layers of Nafion were annealed at 40°C for 2 hours and then for 15 minutes at 120°C to harden them. Polyaniline (PANI) layers of thicknesses of 100 nm and 180 nm were made in a vacuum evaporation process. The whole process was carried out in the residua atmosphere of argon (Ar), in connection with the oxidation of the polymer during the time of its application, which affected the sensing properties of the layers. To achieve the desired quality of the atmosphere in the vacuum chamber, the set-up was rinsed three times with argon. Then, in order to evaporate the water vapor trapped in the PANI, the structure was annealed at 200°C for 10 minutes. The polyaniline application process was made at a temperature of 350–400°C. To obtain the desired thickness, the sublimation process lasted about 45 minutes.

The detector layer (**Figure 3**) of the (RR)—P3HT type polymer with a thickness of ~350 nm, in the empty space of one of the delay lines of the quartz module with SAW was created. The thickness using the atomic force microscope (AFM) profile analysis was estimated. A field fragment polymer plate to use a suitably designed mask was exposed. Through the open window spraying method (nozzle thickness—0.4 mm) a pre-prepared polymer solution (RR)—P3HT was applied. Compressed synthetic air at a pressure of 1 atm. Was used. Solution by dissolving about 1 mg (RR)—P3HT in 1 ml chloroform was prepared. The distance of the nozzle from the substrate during the process was: about 40 mm, settling time was about 3 s (see **Figure 4**) [1, 8].

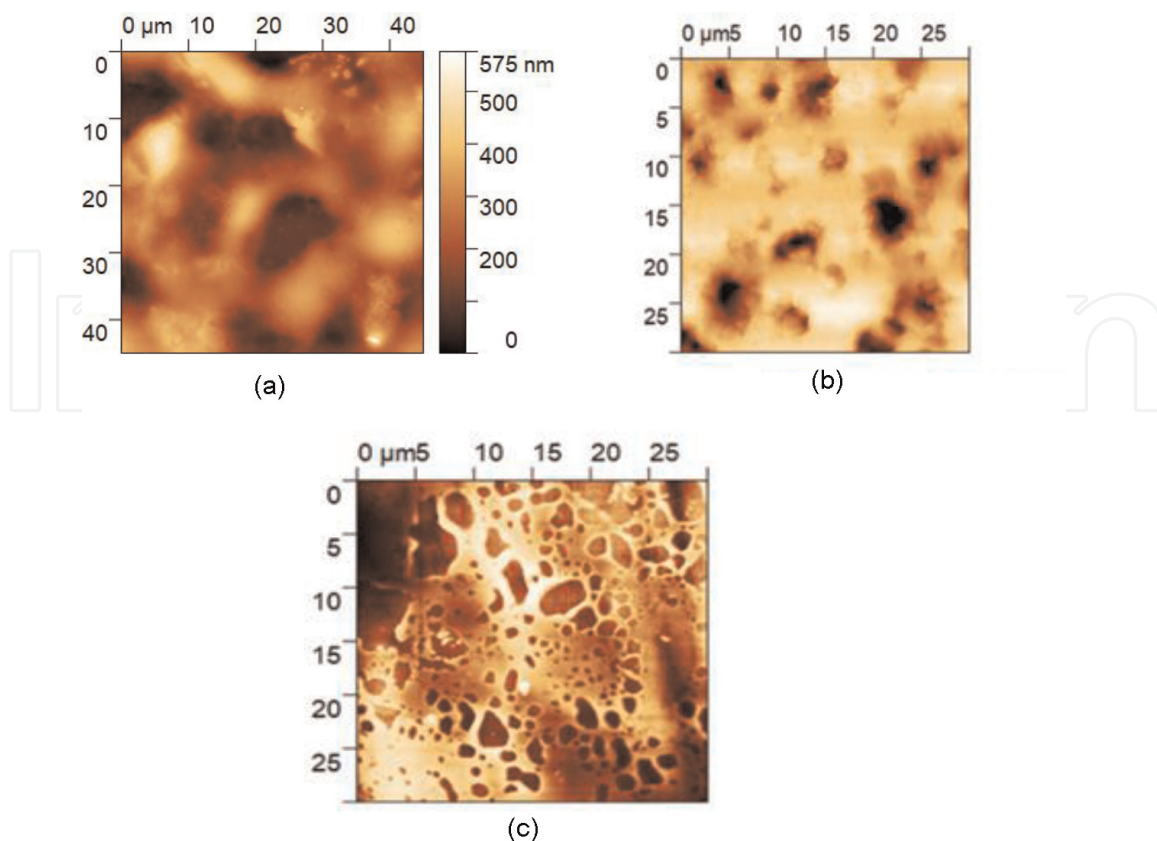


**Figure 3.** Layer topography/morphology (RR) P<sub>3</sub>HT quartz substrate—Fragment of polymer layer (RR)-P<sub>3</sub>HT on quartz crystal from SAW—View under magnification (a), AFM images of the P<sub>3</sub>HT-RR sensing layer measured on a laminate: The polymer surface—resistive detectors research (b) AFM images of the P<sub>3</sub>HT-RR sensing layer on metallization: The polymer surface—Resistive detectors research (c) [1].



**Figure 4.** View of a fragment of the applied polymer layer (RR)-P<sub>3</sub>HT on the quartz crystal of the AFP module. View of the boundary of the formation of a porous layer from the crystal edge visible from above 100x magnification [1].

The sensing mechanism in PANI or PPY (Polypyrrole) and P<sub>3</sub>HT detectors layers is very interesting. The interaction of CO molecules with PANI is primarily of electrical nature. CO is an oxidizing gas—CO molecules attach electrons from the PANI structure. Polyaniline is a p-type semiconductor. The binding of PANI electrons to CO molecules results in an increase in the electrical resistance of the structure (the difference between the concentration of holes and electrons increases). This is manifested by a decrease in the frequency of the measuring resonator and, as a result, a decrease in  $\Delta f$  relative to the situation without CO particles in the atmosphere. In the measurements, the sensing structure was tested for the presence of very low concentrations of CO (5, 10, 15, and 20 ppm) in the synthetic air.

The P3HT contains delocalized  $\pi$  bonds, which permit the easy flow of electrons within the delocalized  $\pi$  system. The relative response of P3HT to analyte species depends on their Lewis acidity or basicity: stronger acids or bases have a larger effect on polymer resistance, with acids decreasing resistance and bases increasing resistance. For DMMP, there is a phosphorous-oxygen double bond. The electronegativity of the oxygen atom is stronger than that of the phosphorus atom, resulting in the increase of the electron density of the oxygen, so DMMP shows alkalescence. The p-type semiconducting behavior of P3HT promotes holes in the valence band of P3HT which play a key role in sensing properties. The DMMP is a strong electron donor which depletes holes from the valence band of P3HT, resulting in an increase of resistance after being adsorbed on the P3HT surface. The number of charge carriers in the P3HT film is increased by the light excitation, resulting in enhanced sensing properties, like sensitivity, the limit of detection, and response time. In addition, for the highly developed surface of the sensing layer deposited on the porous substrate, we obtain more active adsorption sites, and the scheme of the sensing mechanism described above is presented in [15].

### 3. Experimental investigations

In the research, a measuring stand with resonators on acoustic surface waves SAW with a positive feedback loop was used in historical measurements (**Figure 2a**). The system consists of two identical delay lines—DLs (or resonators). One of the delay lines (or resonator) is isolated from the influence of the external atmosphere. The second line (resonator) is exposed to an external gas environment. Changes in the chemical composition of the atmosphere change the resonance frequency of the active line (resonator). At the output of the set-up (DLs or resonators), their high-frequency signals are electronically mixed. The frequency of the delay line without the structure of the detectors was 43.60 MHz, while the sensing structure was lower from several dozen to even one hundred kHz (as a result of its mass loading by the sensing structure). The normal mode frequency configuration (NMFC) occurs when the measuring frequency ( $f$ ) is lower than the reference ones ( $f_0$ ). In the investigations as mentioned above, the bilayer sensing structures of Nafion+Polyaniline were examined by means of the acoustoelectric method in the NMFC case and the difference frequency  $\Delta f$  is determined as  $f - f_0$  (see **Figures 5 and 6**).

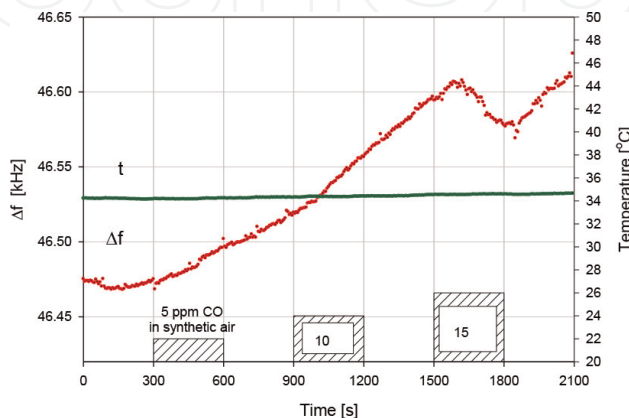


**Figure 5.** Response ( $\Delta f$ ) of the bilayer detector structure PANI (100 nm) + Nafion, to CO gas (5, 10, 15 ppm) in air,  $T = 34^\circ\text{C}$ .

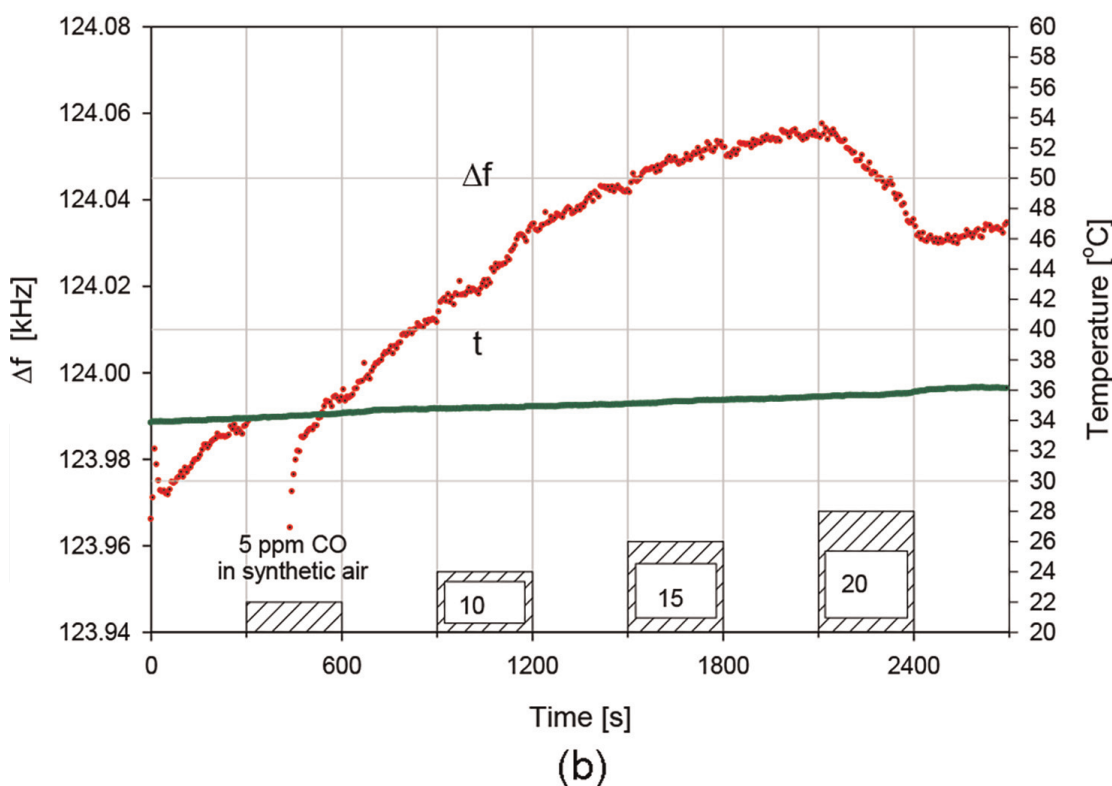
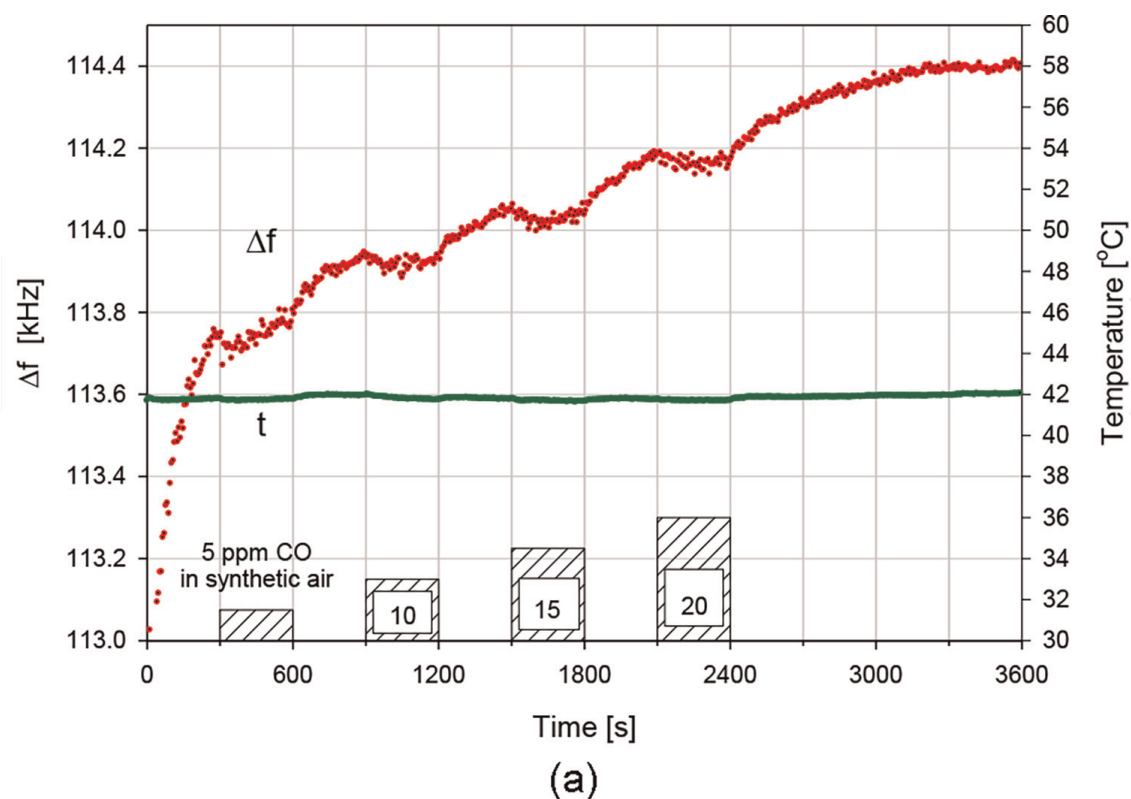


**Figure 6.** Response ( $\Delta f$ ) of the bilayer detector structure PANI (180 nm) + Nafion, and CO gas (5, 10, 15, 20 ppm),  $T = \sim 42^\circ\text{C}$  (a), response ( $\Delta f$ ) of the detector layer PANI (180 nm) + Nafion, CO gas (5, 10, 15, 20 ppm),  $T = \sim 35^\circ\text{C}$  (b) [2].

The results of the studies prepared for the numerical acoustoelectric analysis (NNA) studies for the PANI layer below were shown.

The collective responses ( $\Delta f_{\text{max}} - \Delta f$ ) /  $\Delta f_{\text{max}}$  SAW detector on CO gas at thicknesses 100 nm and 180 nm (PANI), for the concentration from 5 to 15 ppm in



synthetic air at a temperature of 34° C (100 nm) and 35° C (180 nm) in **Figure 7** were showed (**Figure 8**) [2].

The work presents comparative measurements for a polymer layer based on Polypyrrole. The results of the experiment below were shown (**Figure 9**).

Comparison of the detection properties of Polyaniline + Nafion layers (film thickness of 100 nm and 180 nm) and Polipirol layer (thickness 80 nm) of the concentration of 25 ppm, 37.5 ppm, 50 ppm in **Figure 10** were shown. It is clear that the Polypyrrole layers will be suitable for the measurement of higher concentrations.

The main aim of researching selected detector structures with a surface acoustic wave was an empirical verification of the response with numerical analysis. We must emphasize that performing empirical research was possible within limits because of

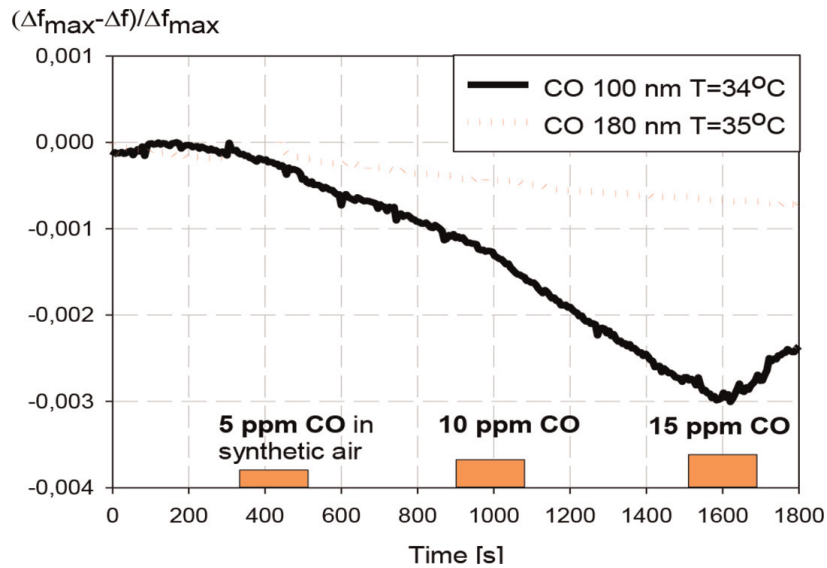


**Figure 7.** Relative changes of the response of a detector normed to maximum differential frequency for each layer PANI +Nafion: 100, 180 nm, CO gas (5, 10, 15 ppm), in synthetic air—measuring system **Figure 2a**.

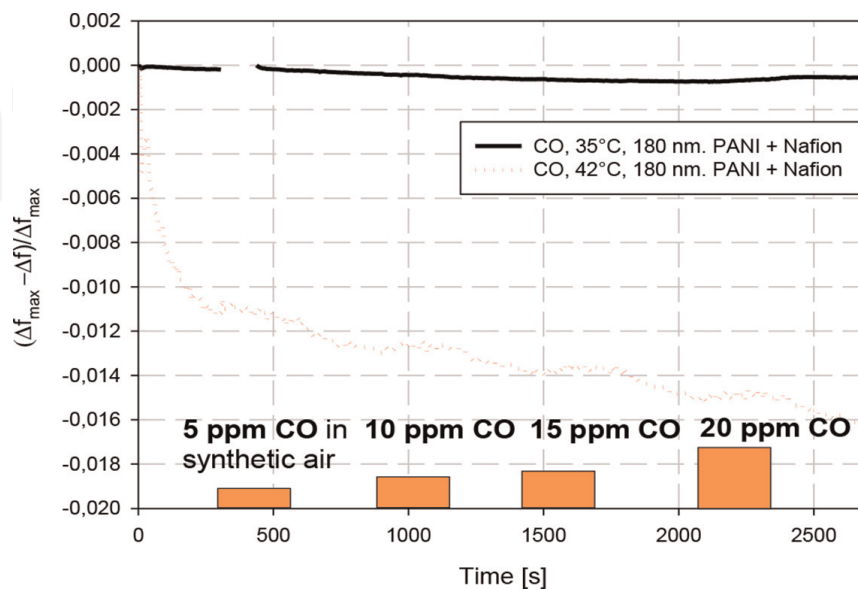


**Figure 8.** Relative changes of the response of a detector normed to maximum differential frequency for PANI+Nafion 180 nm, CO gas (5, 10, 15, 20 ppm), at temperature: 35°C and 42°C—measuring system **Figure 2a**.

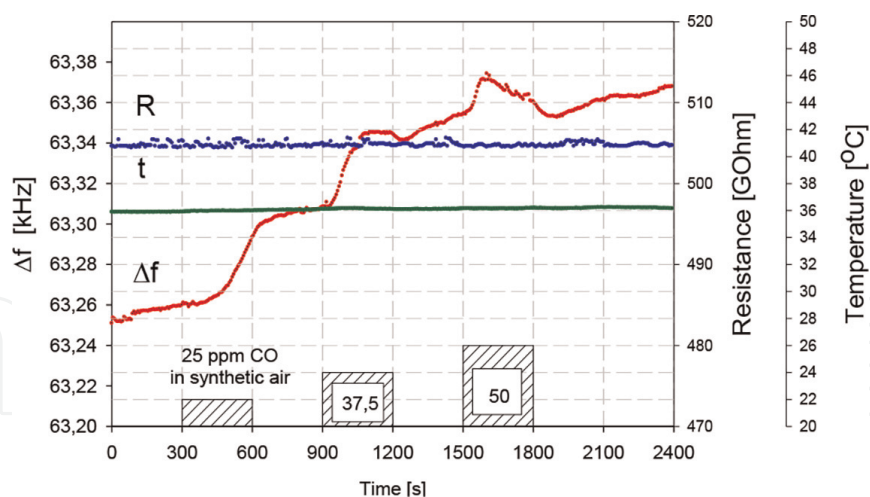


**Figure 9.**  
 Acoustical response ( $\Delta f$ ) and resistance response ( $R$ ) of the detector layer PPy (Polypyrrole 80 nm), CO gas (25, 37.5, 50 ppm),  $T = 36^\circ\text{C}$ —measuring system **Figure 2a**.

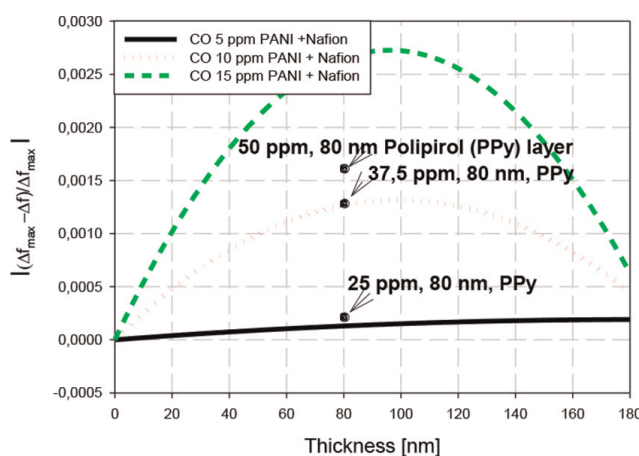


**Figure 10.**  
 A comparison of the detection properties of PANI + NAFION with empirical results of Polypyrrole layer (80 nm) at temperature =  $35^\circ\text{C}$ —measuring system **Figure 2a**.

the wide range of work and the complex technological processes connected with the practical feasibility of the detector structure [1, 16].

A practical system for testing the acoustic-electrical properties of polymer layers based on (Regio-Regular)-P3HT in **Figure 11** was shown.

Empirical results for illuminating LEDs (200 mA) with different wavelengths of the layer (RR)-P3HT are shown in **Figure 12**. The research system from **Figure 2b** was used. The measuring system uses diodes—1 W SMD 350 mA ProLight Opto.

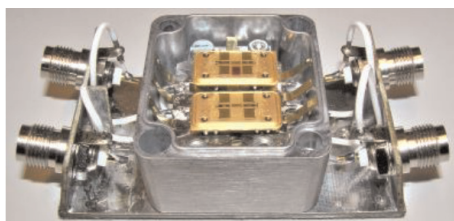


**Figure 11.**  
 The practical implementation of the invention of the patent no. PL 230526 B1—A measuring chamber for testing using SAW detectors—measuring system **Figure 2b**.

Results of measurements DMMP in interaction with polymer layer RR-P3HT illuminated with a diode light of 200 mA in the form of a histography are shown in **Figure 13**.

In order to optimize numerically and compare the experiment with the theory, the results of the experiment depending on the concentration were normalized as follows in **Figure 14**.

Three measurement series were made. The diodes were driven with 100, 200, 300 mA current. The layer was additionally activated by a small incandescent lamp with white light (with a maximum of about 750 nm) and different illuminance (see **Figure 13**). Exposure time was about 10 min for each 100, 200, and 300 mA current.

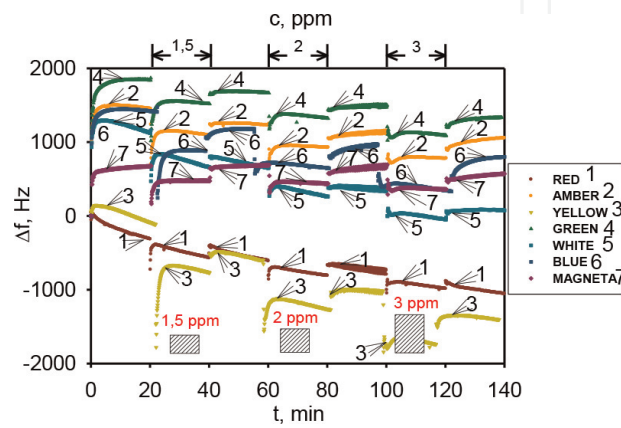


**Figure 12.**

Experiment—Detector layer (RR)-P3HT, thickness 500 nm, gas DMMP (1.5; 2; 3 ppm, illumination by diode 200 mA (selected wavelengths) relative change of velocity vs. time (concentration)—measuring system **Figure 2b**.

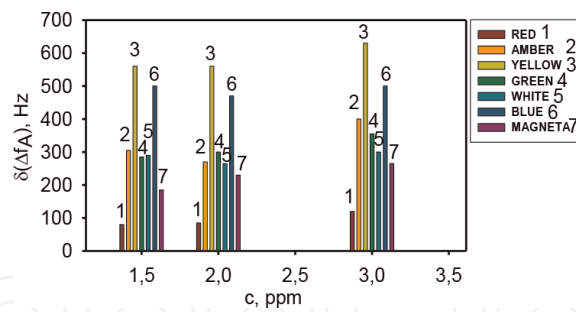


**Figure 13.**

Experiment—Layer (RR)-P3HT, thickness 500 nm, gas DMMP (1.5; 2; 3 ppm, illumination by diode 200 mA (selected wavelengths)—Histogram—relative change of velocity vs. time (concentration)—measuring system **Figure 2b**.

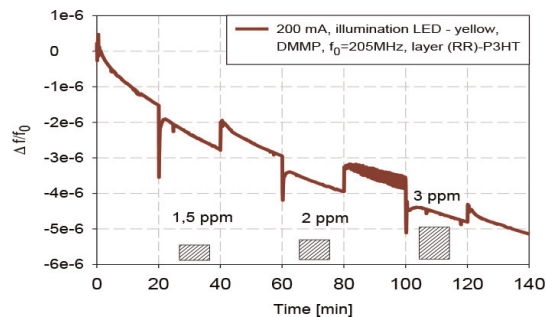


**Figure 14.**

Experiment—Layer (RR)-P3HT, thickness 500 nm, gas DMMP (1.5; 2; 3 ppm, illumination by diode 200 mA (yellow light) normalized results relative change of velocity vs. time (concentration)—measuring system **Figure 2b**.

In order to optimize numerically and compare the experiment with the theory, the results of the experiment were normalized as follows in **Figure 14**—depending on the concentration. Results with a DMMP concentration of 2 ppm in the air were shown.

#### 4. Numerical analysis (NNA) of the acoustoelectric interaction in the sensing layer in the steady state conditions

The acoustic-electric effect depends on the electrical charge profile distribution in the sensing layer on the absorbed gas particles' distance from the surface acoustic waveguide.

To determine the response of the detectors common impedance was designated. Impedance includes information about the profile of the concentration of gas molecules in the layer and has been implemented into the Ingebrigtsen formula [23]. This enables describe relative change velocity surface acoustic waves in steady state and transient mode. Analytical expressions clearly define the model of the SAW detectors. Based on this model numerical analysis detector's response was made. The results of numerical analyzes are shown in the next section.

The analytical model of a SAW gas detector having the described form was used in order to analyze it numerically. In order to analyze such a detector layer in the SAW gas detector we assumed that the film is a uniform stack of infinitesimally thin sheets with a variable concentration of gas molecules (**Figure 15**) and that it influences the electrical conductance [10].

$$\frac{\Delta v}{v_0} = -\operatorname{Re}\left\{\frac{\Delta k}{k_0}\right\}$$

$$= -\frac{K^2}{2} \frac{\left[\sigma_{T_2}(1 + aC_{A,y=0}) + \sum_{i=1}^{n-1} \sigma_{T_2}(y_i) f(y_i, \sigma_{T_2}(y_i))\right]^2}{\left[\sigma_{T_2}(1 + aC_{A,y=0}) + \sum_{i=1}^{n-1} \sigma_{T_2}(y_i) f(y_i, \sigma_{T_2}(y_i))\right]^2 + \left[1 + \sum_{i=1}^{n-1} g(y_i, \sigma_{T_2}(y_i))\right]^2 (v_0 F_S)^2}$$

(1)

where: n—number of sublayers and  $F_S = \epsilon_0 + \epsilon_p^T$ ,  $i = 1, 2, 3, \dots, n$  (the sublayers index),  $\Delta v/v_0$  and  $\Delta k/k_0$  relative changes of velocity and wave vector of SAW,

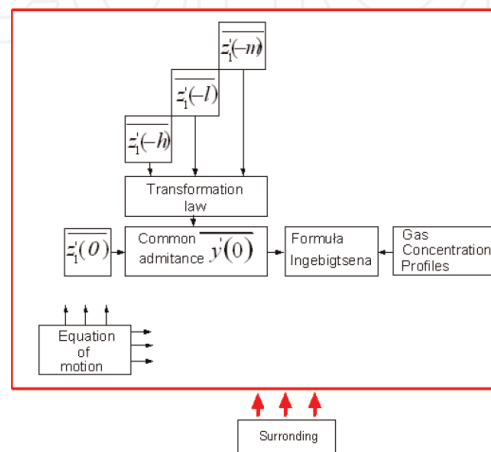


**Figure 15.**  
 Schematic diagram of the SAW detector model [2].

respectively,  $\sigma_0$ —electrical conductivity of sensing layer in air,  $K^2$ —coefficient of electromechanical coupling,

$$\sigma(y_i) = \sigma_0 [1 + a \cdot C_A(y_i)] \quad (2)$$

where:  $a$ —sensitivity coefficient of the sensing layer [1/ppm].

In the expression (1) the functions  $f(y_i, \sigma(y_i))$  and  $g(y_i, \sigma(y_i))$  are the results of the transformation of the individual sublayer on the surface of a detector waveguide (**Figure 15**) and it has the form:

$$f(y_i, \sigma(y_i)) = \frac{1 - [\operatorname{tgh}(ky_i)]^2}{[1 + \operatorname{tgh}(ky_i)]^2 + \left[ \operatorname{tgh}(ky_i) \cdot \frac{\sigma(y_i)}{\varepsilon_0 v_0} \right]^2} \quad (3)$$

and

$$g(y_i, \sigma(y_i)) = \frac{1 - [\operatorname{tgh}(ky_i)]^2}{[1 + \operatorname{tgh}(ky_i)]^2 + \left[ \operatorname{tgh}(ky_i) \cdot \frac{\sigma(y_i)}{\varepsilon_0 v_0} \right]^2} \quad (4)$$

The conductivity of the detector layer depends on the temperature:

$$\sigma_{T_2} = \sigma_{T_1} \exp\left(\frac{E_g}{2k_B} \cdot \frac{T_2 - T_1}{T_1 T_2}\right) \quad (5)$$

where  $T_1 = 300$  K,  $\sigma_{T_1} = \sigma_0$  are the conductance of the layer, respectively, at temperature the  $T_1$  and  $T_2$ ,  $k_B$ —the Boltzmann constant,  $v_0$ —SAW velocity,  $k$ —acoustic wave number ( $k = 2\pi/\lambda$ ),  $E_g$ —the width of the energy gap of detector layer material. The expressions (1, 3, 4) make it possible to determine the use of the iteration method response of the surface acoustic wave in the steady-state ( $t \rightarrow \infty$ ).

For the selected parameters (thickness, concentration, temperature, sensitivity  $a$ , and conductivity) of bilayer sensor structure (Nafion+Polyaniline), the numerical analysis were made and the influence of carbon monoxide gas concentration on detection response was determined.

**Figure 16** presents the numerical analysis detector response depending on the thickness detector layer. From the analysis, it follows that the optimum thickness is approx. 90 nm. The software was written in Python. In the range of thicker layers

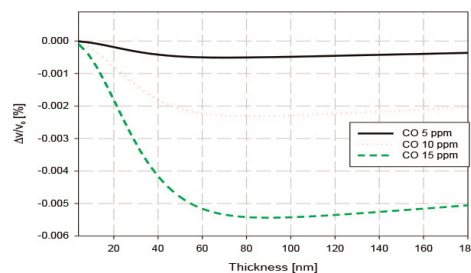


**Figure 16.** Changes of velocity (relative) vs. thickness from 2 nm to 180 nm, Nafion+Polyaniline. Assumed in the analysis: Sensitivity coefficient  $a = -4.25 \text{ ppm}^{-1}$ ,  $\sigma_s = 2 \times 10^{-12} \text{ S}$ ,  $M = 28 \text{ g/Mol}$  (CO), concentration: 5, 10, 15 ppm. Numerical results.

above 180 nm interaction decreases, which confirms obtained empirical results. From the characteristic, it follows that for the small concentration (below 5 ppm) measurements of carbon monoxide using an SAW detector for the layer above 180 nm and thicker will be useless (measurement temperature of 35°C, see **Figures 5, 6a**). This fact very explicitly confirms the experiment mentioned above for thickness layer of 180 nm and at the temperature of 35°C.

The numerical analysis of the influence of the CO concentration on the response of the detector in a layer thickness of 180 nm for a temperature of 35° C and 42° C (**Figure 6b**) was made (**Figure 17**).

A separate place is devoted to researching the temperature properties of the layer. It is important here to note that the selection of the operating temperature of the detector depends not only on the type of detector layer but also on the porosity and roughness (**Figure 18a and b**). Temperature change also allows to determine the operating point of the detector and also has an impact on the speed of response and recovery of the detector layer. Changing the operating point of the detector by increasing the temperature from 35°C to 42° C, should increase the detection properties of the detector in accordance with the experiment (**Figure 6a and b**). The effect of temperature on the response of the gas detector is also confirmed by the analysis of the properties of the temperature detector (**Figure 8**). The numerical analysis of the influence of the temperature on the response of the detector in a layer thickness of 180 nm for a temperature of 35°C (308 K) and 42°C (315 K) was made (**Figure 19**). Numerical analysis shows that based on the numerical model of a gas detector with a layer of Nafion + Polyaniline gas impact in the case of measuring the temperature increase of 35–42°C will result in a marked increase in the detector response.

The results of numerical analysis (**Figure 19**) coincide approximately with the results of the experiment (see **Figures 5–8**).

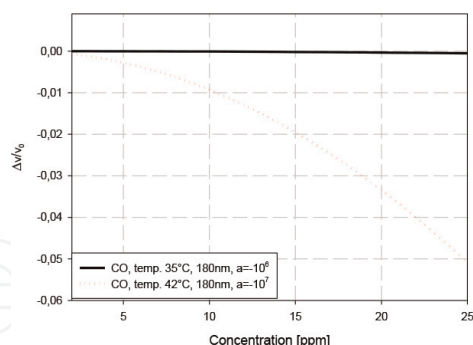


**Figure 17.** Changes of velocity (relative) vs. concentration from 2 to 25 ppm in synthetic air, Nafion+polyaniline at temperatures 35°C and 42°C. assumed in the analysis:  $H = 180 \text{ nm}$  (thickness), sensitivity coefficient  $a = -10^6 \text{ ppm}^{-1}$  ( $T = 35^\circ\text{C}$ ),  $a = -10^7 \text{ ppm}^{-1}$  ( $T = 42^\circ\text{C}$ ),  $\sigma_s = 2 \times 10^{-12} \text{ S}$ ,  $M = 28 \text{ g/Mol}$  (CO). Numerical results.

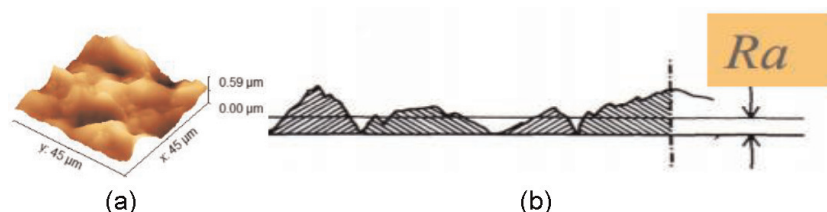


**Figure 18.** The polymer layer (RR)-P3HT surface 3D-AFM view (a) graphic illustration of the average profile radius (b).

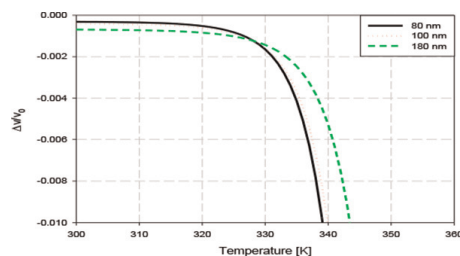


**Figure 19.** Changes of velocity (relative) vs. temperature from 300 K to 344 K, Nafion+polyaniline, assumed in the analysis:  $A = -1 \text{ ppm}^{-1}$ ,  $\sigma_s = 2 \times 10^{-12} \text{ S}$ ,  $M = 28 \text{ g/Mol}$  (CO), concentration 5 ppm, thickness 80, 100, 180 nm. Numerical results.

The sensitivity of sensing structures to external gas atmospheres depends on the temperature of the structure. The problem of the structure temperature is also important in the aspect of “detoxifying” its electrical properties after measurements. Our previous research [2] shows that detoxification is much more effective at elevated temperatures. On the other hand, however, the elevated temperature affects the mechanical degradation of the structure and causes irreversible changes in its physicochemical properties. This problem is particularly important when the sensing layers are made of organic semiconductors. Polyaniline and Nafion are organic semiconductors. In order not to destroy the examined structures, the measurements were made at relatively low temperatures: 35°C (308 K) and 42°C (315 K).

Analyzes for the sarin simulator—DMMP gas was also performed. The roughness of the polymer [25] detector layer for the average height of the layer profile from 60 nm to 960 nm (max. average height of the layer profile) theoretically and numerically was performed. The thickness using the atomic force microscope (AFM) profile analysis was estimated too. The acoustoelectric interaction of the surface wave with charge carriers distributed in the detector layer according to the profile resulting from the diffusion of gas molecules from the surrounding atmosphere was analyzed numerically in the Python programming environment, using the expression (1)–(5) [10]. The results of the numerical analysis can be the basis for the optimization of the layer parameters in terms of the maximum sensitivity of the detector. **Figures 20, 21, and 22–24** show exemplary results of the numerical analysis.

The best results in the range of 60–960 nm thicknesses have been achieved. In **Figure 20** analysis for a polymer (RR)-P3HT was performed. For the assumed DMMP gas ambient parameters (temperature, concentration 3 ppm) and layer parameters

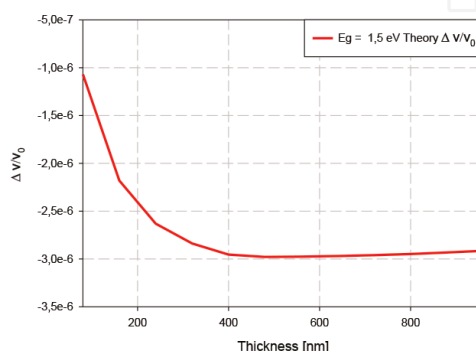


**Figure 20.** Changes of velocity (relative) vs. thickness, from 80 nm to 960 nm, layer (RR)-P3HT, gas DMMP:  $\sigma_s = 5 \times 10^{-4} \text{ S}$ ,  $M = 124.08 \text{ g/Mol}$ ,  $K_2/2$  (quartz) = 0.09%,  $C = 3 \text{ ppm}$ .

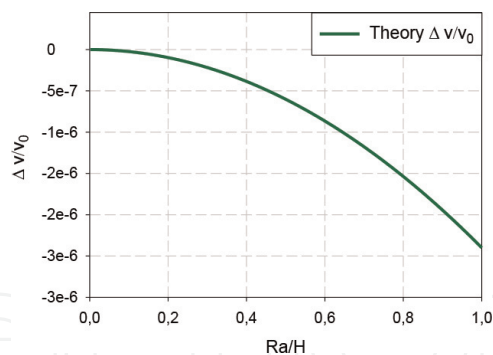


**Figure 21.** Changes of velocity (relative) vs. roughness, temp. 305 K (32°C), (RR)-P3HT,  $a = 1 \text{ ppm}^{-1}$ ,  $\sigma_s = 5 \times 10^{-4} \text{ S}$ ,  $D_K = 10^6 \text{ nm}^2 \text{ s}^{-1}$ ,  $E_g = 2.7 \text{ eV}$ ,  $M = 124.08 \text{ g/Mol}$ , DMMP concentration: 2 ppm, thickness 500 nm ( $H$ ),  $K_2/2$  (quartz) = 0.09%, measurement AFM  $R_a = 76 \text{ nm}$ .

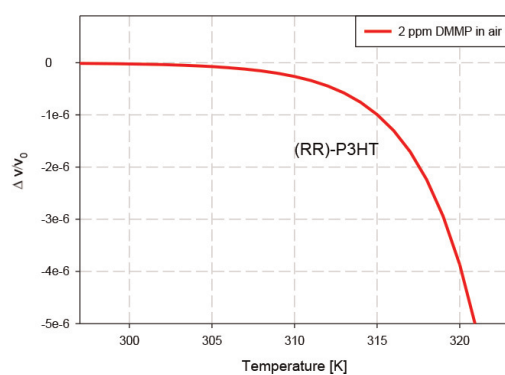


**Figure 22.** Temperature range: 293–322 K (20–49°C)—Curve (theoretical numerical calculations):  $\sigma_s = 5 \times 10^{-4} \text{ S}$ ,  $M = 124.08 \text{ g/Mol}$ ,  $K_2/2$  (quartz) = 0.09%,  $C = 2 \text{ ppm}$ .

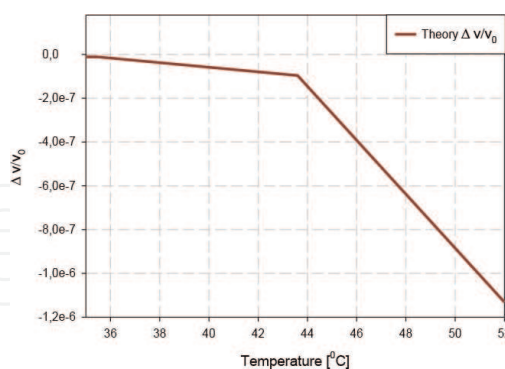


**Figure 23.** Curve (theoretical numerical calculations) for parameters:  $\sigma_s = 5 \times 10^{-4} \text{ S}$ ,  $M = 124.08 \text{ g/Mol}$ ,  $K_2/2$  (quartz) = 0.09%,  $C = 2 \text{ ppm}$ .

(sensitivity, conductivity, diffusion parameters, substrate—quartz), the graph shows the value of about  $3 \times 10^{-6}$  for a layer with a thickness of 500 nm. The changes resulting from the numerical model are at a relative level of changes of the order of  $10^{-6}$ . The results shown in **Figure 20** show that there is an optimal thickness of the detector layer for which the acoustoelectric impact (change in the velocity of the acoustic wave) is the greatest. Qualitatively, the existence of an optimal layer thickness was confirmed empirically in Ref. [7, 8].



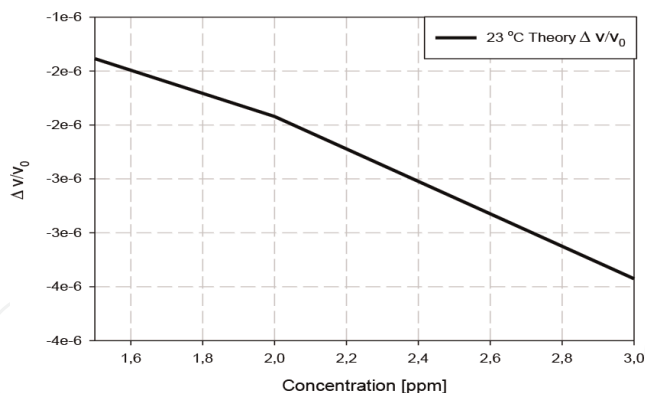


**Figure 24.**

Changes (relative) of velocity vs. concentration, temp. 305 K (32°C), (RR)-P3HT,  $a = -1.75 \text{ ppm}^{-1}$ ,  $\sigma_s = 5 \times 10^{-4} \text{ S}$ ,  $DK = 10^6 \text{ nm}^2 \text{ s}^{-1}$ ,  $E_g = 2 \text{ eV}$ ,  $M = 124.08 \text{ g/Mol}$ , gas DMMP, thickness 500 nm,  $K_2/2$  (quartz) = 0.09%.

The thickness of the layer affects the response of the detector layer, also in this case. In our case, we identified the height of the layer with the average radius of the detector layer profile. This is a particularly favorable circumstance because in the perturbation theory, the concept of surface conductivity is used. The following graph was obtained by equating the average radius of the  $R_a$  layer with the thickness of the layer  $\sigma_s = \sigma R_a$ . This fact gave our considerations a further direction enabling the development of a mathematical model to take into consideration roughness. In this case, most of the volume of the layer is close to the surface of the piezoelectric layer of the quartz base. The diffusion of larger molecules is not difficult, however, in layers of greater thicknesses above about 650 nm, the interaction is not as strong as in smaller ones, eg. 100 nm. The electrical conductivity of the deeper parts of the layer changes, and their contribution to the detector response is significant. In the case of detectors based on polymer layers, the shape of the surface and its roughness are significant. The above characteristics of the detector response depending on the average radius of the layer's profile were shown (**Figure 18**). The average radius of the  $R_a$  layer profile by the height of the H-layer for the better presentation was normed ( $R_a/H$ —**Figure 21**). In the case of the average profile radius  $R_a$  of 0, the layer “disappears”, boundary conditions correspond to the lack of interaction of the analyte with the detector layer. In the case when the average radius of the  $R_a$ —layer profile reaches the height of the maximum H. This is a theoretical case when we have an ideal detector layer in the image of a “rectangular”—and the surface that is not rough—a theoretical case. Therefore, the roughness has decisive for the response of the DMMP gas detector based on the optic layer using (RR)-P3HT and this aspect will be developed in further studies. In the case of DMMP, the optimal layer thickness is approx. 500 nm. These analyzes were carried out for other analytes, such as:  $\text{H}_2$ ,  $\text{CO}_2$ ,  $\text{NO}_2$ ,  $\text{NH}_3$ . Numerical NNA analysis also showed the existence of an optimal thickness at which the interaction is greatest. The optimal thickness for  $\text{LiNbO}_3$  (piezoelectric) layer and interaction with gases  $\text{H}_2$ ,  $\text{CO}_2$ ,  $\text{NO}_2$ ,  $\text{NH}_3$  was approx. 100 nm [9]. As a rule, the diffusion of larger molecules is difficult, additional in layers of higher thicknesses, the entire volume of the layer is not saturated. However, in the case of polymers, it is the other way round. The electrical conductivity of the deeper parts of the layer also changes, so their contribution to the detector response is significant. This state describes the solution of the general diffusion equation for polymers [26].

The results of the experiment to the theory were compared. **Figure 22** shows theoretical numerical analysis in the temperature range of about 293–322 K. Below a

comparison of numerical calculations based on the assumed layer model with empirical measurements was made. Good consistency of row magnitude was achieved. The results of the experiment coincide with the theory and are convergent. The calculations for a DMMP concentration of 2 ppm were made.

In **Figure 24** the theoretical dependence of the detector response depending on the concentration in the range from 1 to 3 ppm was shown. The results of empirical research concern the concentration of 1.5–3 ppm and at 32°C were made. All tests on a piezoelectric substrate made of quartz were done.

## 5. Summary

In research layers (PANI) for different thicknesses: 100, 180 nm, Nafion approx. 300 nm were prepared. The main target was to research the interaction of carbon monoxide and a layer of PANI change were measured. Influence the temperature on the bilayer structure of Nafion+Polyaniline at  $T = 35^\circ\text{C}$  and  $T = 42^\circ\text{C}$  were examined. Visible effects were observed at low CO concentrations—5 ppm. During the experiment, representative samples of the PANI with a Nafion layer thicknesses of 100 and 180 nm were investigated. Very interesting properties were examined at layer 180 nm depending on the interaction temperature. Very clearly and a sharp rise detection of carbon monoxide properties as a result of the growth of the temperature of about  $7^\circ\text{C}$  (temperature change from  $35^\circ\text{C}$  to  $42^\circ\text{C}$ ) was observed. Exactly ambient temperatures were measured. Empirical results with layer basis on PANI + Nafion (100, 180 nm) compared with Polypyrrole detector layer (thickness  $\sim 80$  nm). It is useful to measure a higher level of the concentration of CO above 25 ppm. Extensive numerical analyses on CO of the SAW response parameter like: thickness, concentration, and temperature at low concentrations (5 ppm) were conducted. Numerical researches were performed in a steady state. As shown above, PANI and PPy nano-layers have a lot of valuable physical properties useful for applications in various fields of science. These materials are used in medical and biological applications, eg. for the detection of both chemicals, e.g. the selected metal cations, lactic acid as well as biological samples—tumor cells. Polyaniline nano-layers can develop a detector that can detect lactic acid in the range of physiological concentrations informing about the different types of diseases. Empirical studies can observe specific changes in the electrical conductivity of micro and PANI nanolayers in contact with tumor cells and healthy [13].

Detector studies of photoconductive (RR)-P3HT were performed as a potential material for detecting trace amounts of DMMP compound vapors (2 ppm) in air using the SAW method. Polymer (RR)-P3HT possesses significant sensitivity to trace amounts of DMMP, only when additional white light was used. Increasing the light flux also causes the sample temperature to rise and to obtain larger frequency variations (130–300 Hz) for the same concentration of 2 ppm DMMP in the air. Estimated response and regeneration times for this DMMP concentration are respectively 10–20 sec. and 7 min [1]. Extensive NNA of the SAW detector response depending on parameters: concentration, roughness, temperature, and thickness were conducted. Numerical research was performed in a steady state. NNA was performed using proprietary software written in Python. The layer thickness decides the maximum range of the detected gas concentration [10].

Also, the choice of the temperature of the polymer detector is important—the optimal work temperature depends on the type of the detector layer and its roughness. The change in temperature allows to determine the point of detector work, and has

also an impact on the speed of its response and the recovery time of the sensing properties of the detector layer [9]. Empirical results of a SAW detector with (RR)-P3HT were achieved for three thicknesses ( $\sim 100, \sim 350, \sim 550$  nm) of the layers. The main target was to verify empirically the analytical model of the SAW gas detector affected by: 2, 3 ppm DMMP in the air. Empirical results confirmed the usefulness of the elaborated analytical model for the investigation of the SAW detector in the design stage. In particular, the influence of the concentration and thickness (existing optimal thickness) was confirmed. The essential parameter of the polymer detector is the roughness of the sensing layer—under investigation.

The results of numerical acoustoelectric analysis of the SAW detector investigations confirmed theoretical were showed. Different sources of light (different of wavelengths light LED, see **Figure 13**) were selected and different wavelengths (histogram) were checked.

The study has shown that the parameters of the detector layer for the SAW detector should be individually adjusted, according to the type of the detected gas and the applied sensing layer. The exposure time of polymer layers was also empirically selected for about 10 min for each current value of 100, 200, 300 mA and the detector layer was illuminated with LED light of different wavelengths and different light energy. From the tests, the best results for yellow light: 76.6–87.4 [lm] and wavelength = 560 nm were obtained. The author's main goal was to numerically analyze phenomena based on empirical investigation and to create a predictive model that would show the tendency of changes before they appear. Extensive numerical analyses of the SAW detector response depending on parameters like: concentration, roughness, temperature, and thickness were conducted. Numerical investigation were performed in the steady state conditions in Python.

## **Acknowledgements**

Authors would like to thank the Presidents: Wojciech Wajda WASKO SA (innovation technology and research Enterprise) and Michał Mental ENTE Ltd. (the newest electronic factory) for the possibility of work: theoretical, analytical, numerical, and investigation works as well as participation in R & D works financed from the NCBiR grants. The authors of the paper thank Paulina Powroźnik (intensive research), Anna Kaźmierczak-Bałata (morphology), Maciej Setkiewicz (performance sensing layer and technology), Mirosław Magnuski (electronic design of appliance high frequency and patent) Monika Hejczyk—President Foundation—The Academy of Creative Development (statut support for science) for his help in the experimental investigations.

IntechOpen

### **Author details**

Tomasz Hejczyk<sup>1</sup>, Jarosław Wrotniak<sup>2</sup> and Wiesław Jakubik<sup>3\*</sup>

1 The Academy of Creative Development—The Foundation, Marklowice, Poland


2 Institute of Electronics, Silesian University of Technology, Gliwice, Poland

3 Institute of Physics CSE, Silesian University of Technology, Gliwice, Poland

\*Address all correspondence to: [wieslaw.jakubik@polsl.pl](mailto:wieslaw.jakubik@polsl.pl)

### **IntechOpen**

---

© 2022 The Author(s). Licensee IntechOpen. This chapter is distributed under the terms of the Creative Commons Attribution License (<http://creativecommons.org/licenses/by/3.0>), which permits unrestricted use, distribution, and reproduction in any medium, provided the original work is properly cited. 

## References

- [1] Wrotniak J, Jakubik W, Powroźnik P, Stolarczyk A, Magnuski M. Akustyczne badania polimeru typu RR-P3HT do wykrywania DMMP w powietrzu (in polish). *Przegląd Elektrotechniczny*. 2018;**94**(6):70-73. DOI: 10.15199/48.2018.06.12
- [2] Hejczyk T, Pustelny T. Analysis of the saw system with the PANI + Nafion sensing structure for detection of low concentration carbon monoxide. *Archives of Acoustics*. 2020;**45**(4): 681-686. DOI: 10.24425/aoa.2020.135274
- [3] Matsumaga N, Sakai G, Shimanoe K, Yamazoe N. Diffusion equation-based study of thin film semiconductor gas sensor-response transient. *Sensors and Actuators B*. 2001;**83**:216-221
- [4] Matsumaga N, Sakai G, Shimanoe K, Yamazoe N. Formulation of gas diffusion dynamics for thin film semiconductor gas sensor based on simple reaction-diffusion equation. *Sensors and Actuators B*. 2003;**96**:226-233
- [5] Hejczyk T, Pustelny T, Wszolek B, Jakubik W. Numerical analysis of sensitivity of SAW structure to the effect of toxic gases. *Archives of Acoustics*. 2016;**41**(4):747-755. DOI: 10.1515/aoa-2016-0072
- [6] Pustelny B, Pustelny T. Transverse acoustoelectric effect applying in surface study of GaP: Te(111). *Acta Physica Polonica A*. 2009;**116**(3):383-384. DOI: 10.12693/APhysPolA.116.383
- [7] Hejczyk T, Urbanczyk M, Pustelny T, Jakubik W. Numerical and experimental analysis of the response of a SAW structure with WO<sub>3</sub> layers an action of carbon monoxide. *Archives of Acoustics*. 2015;**40**(1):19-24. DOI: 10.1515/aoa-2015-0003
- [8] Hejczyk T, Wrotniak J, Magnuski M, Jakubik W. Experimental and numerical acoustoelectric investigation of the new SAW structure with (RR)-P3HT polymer in DMMP detection. *Archives of Acoustics*. 2021;**46**(2):313-322. DOI: 10.24425/aoa.2021.136585
- [9] Hejczyk T, Urbańczyk M. Numerical optimization of structures SAW gas sensors. *Acta Physica Polonica A*. 2013; **124**(3):432-435. DOI: 10.12693/APhysPolA.124.432
- [10] Urbańczyk M. *Sensors with Surface Acoustic Wave—Monograph*. Vol. 213. Gliwice (in Polish): SUT; 2011
- [11] Pustelny T, Opilski A, Pustelny B. Determination of some kinetic parameters of fast surface states in silicon single crystals by means of surface acoustic wave method. *Acta Physica Polonica A*. 2008;**114**(6A):A183-A190
- [12] Sakiewicz P, Nowosielski R, Babilas R, Gąsiorek D, Pawlak M. FEM simulation of ductility minimum temperature (DMT) phenomenon in CuNi25 alloy. *Journal of Achievements in Materials and Manufacturing Engineering*. 2013;**61**(2):274-280
- [13] Michalska A. *Polyaniline Micro- and Nanostructures for Biomedical Applications*. PhD Thesis (in Polish); 2011
- [14] Hejczyk T, Kamiński G, Ogaza R. Patent no PL 229696 B1, Application of the Hybrid Sensor with Acoustic Surface Wave [in Polish]. 2018. pp. 2-5
- [15] Powroźnik P, Jakubik W, Kaźmierczak-Bałata A. Detection of organophosphorus (DMMP) vapour using phthalocyanine-palladium bilayer

- structures, EUROSENSORS. *Procedia Engineering*. 2015;**120**:368-371. DOI: 10.1016/j.proeng.2015.08.640
- [16] Magnuski M, Wrotniak J. Patent no PL 230526 B1, System for detecting chemical compounds in gaseous atmospheres, with a sensor using surface acoustic waves (SAW). *Polis*. 2018;2-4. P.419823
- [17] Jasek K, Miluski W, Pasternak M. New approach to saw gas sensors array response measurement. *Acta Physica Polonica A*. 2011;**120**(4):639-641. DOI: 10.12693/APhysPolA.120.639
- [18] Pustelny T, Procek M, Maciak E, Stolarczyk A, Drewniak S, Urbanczyk M, et al. Gas sensors based on nanostructures of semiconductor ZnO and TiO<sub>2</sub>. *Bulletin of the Polish Academy of Sciences: Technical Sciences*. 2012;**60**(4):853-859
- [19] Kawalec A, Pasternak M. Microwave humidity sensor based on surface acoustic wave resonator with nafion layer. *IEEE Transactions on Instrumentation and Measurement*. 2008;**9**(57):2019-2023
- [20] Kawalec A, Pasternak M, Jasek K. Measurements results of SAW humidity sensor with nafion layer. *European Physical Journal: Special Topics*. 2008; **154**:121-126
- [21] National Research Council. *Acute Exposure Guideline Levels for Selected Airborne Chemicals*. Washington, DC: The National Academies Press; 2003
- [22] Yoo R, Kim J, Song MJ, Lee W, Noh JS. Nano-composite sensors composed of single-walled carbon nanotubes and polyaniline for the detection of a nerve agent simulant gas. *Sensors & Actuators, B: Chemical*. 2015; **209**:444-448. DOI: 10.1016/j.snb.2014.11.137
- [23] Auld BA. *Acoustic Fields and Waves*. Vol. 2. New York: Wiley; 1973. pp. 271-290
- [24] Long Y, Wang Y, Du X, Cheng L, Wu P, Jiang Y. The different sensitive behaviors of a hydrogen-bond acidic polymer-coated SAW sensor for chemical warfare agents and their simulants. *Sensors*. 2015;**15**:18302-18314. DOI: 10.3390/s150818302
- [25] Lee HJ, Park KK, Kupnik M, Oralkan Ö, Khuri-Yakub BT. Chemical vapor detection using a capacitive micromachined ultrasonic transducer. *Analytical Chemistry*. 2011;**83**(24): 934-932. DOI: 10.1021/ac201626b
- [26] Crank J. *The Mathematics of Diffusion*. Oxford: Clarendon Press; 1975. pp. 259-262